Crystal momentum-dependent anisotropy of the Dirac cone in the rectangular carbon allotropes

2014 EPL 107 20003

(http://iopscience.iop.org/0295-5075/107/2/20003)

epl A Letters Journal Exploring the Frontiers of Physics

July 2014

EPL, **107** (2014) 20003 www.epljournal.org
doi: 10.1209/0295-5075/107/20003

Crystal momentum-dependent anisotropy of the Dirac cone in the rectangular carbon allotropes

D. Z. Yang[1], M. S. Si[1,2(a)], G. P. Zhang[2] and D. S. Xue[1(b)]

[1] *Key Laboratory for Magnetism and Magnetic Materials of the Ministry of Education, Lanzhou University Lanzhou 730000, China*
[2] *Department of Physics, Indiana State University - Terre Haute, IN 47809, USA*

received 7 February 2014; accepted in final form 25 June 2014
published online 11 July 2014

PACS 03.65.Pm – Relativistic wave equations
PACS 81.05.Xj – Metamaterials for chiral, bianisotropic and other complex media
PACS 73.20.-r – Electron states at surfaces and interfaces

Abstract – Thanks to the perfect hexagonal lattice, graphene holds an isotropic Dirac cone. This means that the group velocities of charge carriers in the vicinity of Dirac points are isotropic in momentum space. When the lattice structure varies, the Dirac cone will undergo a dramatic change accordingly. This is the case of 6,6,12-graphyne. Due to the rectangular lattice, Dirac cones of 6,6,12-graphyne are anisotropic. To understand its underlying nature, three additional derivates of 6,6,12-graphyne with the rectangular lattice are studied by using an *ab initio* method. Although the existence of a Dirac cone critically depends on the hopping energies within the unit cell, the anisotropy of the Dirac cone is another story. This is because the anisotropy of the Dirac cone describes the relation between carriers' group velocities, and is thus direction-dependent in momentum space. Our study demonstrates that the anisotropy of the Dirac cone is tunable through changing the lattice constants or the lattice ratios in the rectangular carbon allotropes. This will be the focus of future research as the anisotropy of the Dirac cone can be regarded as an information carrier.

Graphene has recently attracted intense attention because of its versatile electronic properties [1]. Owing to the perfect hexagonal lattice composed of two equivalent triangular carbon sublattices, the bands at the K-points, which are the corners of the Brillouin zone, are conical in the proximity of the Fermi level. The mapping of the 3D conical bands shows features like the so-called Dirac cones, where the valence band touches the conduction band. As a result, the charge carriers are massless fermions, which obey the Dirac equation [2]. Many unusual physical phenomena, such as the half-integer quantum Hall effect [3], the Klein paradox or anomalous absence of back scattering [4], high superconductivity [5] and the novel microwave response effect [6], occur. The ultrahigh carrier mobility of the Dirac fermions [7], along with the ability to manipulate the transport through field effect [8] or doping [9], makes graphene a potential candidate for next-generation electronics.

In general, Dirac cones in graphene are isotropic in momentum space [10]. Recently, anisotropic Dirac cones in the rectangular lattice were predicted in 6,6,12-graphyne [11,12] as well as in the semiconductor quantum dots array [13]. This is a big step in the search for anisotropic Dirac materials, in which the propagation of charge carriers will move in one favorable crystalline direction. Such controllable propagation of carriers along certain directions can be regarded as playing the part of the electron's spin orientation [14], which possibly provides the uses in information applications [15].

The finding of intrinsic anisotropy of Dirac cones has been reported in various materials, such as fcc topological insulator BiSb [16], iron-pnictide high-temperature superconductor $BaFe_2As_2$ [17], photonic crystals [18,19], topological insulator [20], and bulk $Sr(Ca)MnBi_2$ [21]. On the other hand, some approaches have been devoted to achieving artifactual Dirac anisotropy, including applying isotropic strain [22,23], external periodic potentials induced by superlattices [24], and external magnetic field [25], constructing heterostructures [26,27] and

(a) E-mail: sims@lzu.edu.cn
(b) E-mail: xueds@lzu.edu.cn

others [28]. Although the mutual competition between hopping energies at different lattice sites critically dominates the Dirac cones themselves [29], the anisotropy of Dirac cones is another story. This is because the anisotropy of Dirac cones describes the group velocities of carriers and thus is crystal momentum dependent. It requires detailed mapping of the Dirac anisotropy in the entire first Brillouin zone. However, systematic investigations of the Dirac anisotropy in momentum space are still lacking.

As a common symmetry, the rectangular lattice with symmetry group *pmmm* can be easily obtained through rearranging the carbon rings in 2D carbon allotropes. It is worth noting that the lattice constant can be further modulated by replacing some of the carbon bonds by certain acetylenic (-C≡C-) linkages, which is indeed fabricated by coupling reactions of precursor molecules on a copper surface in experiment [30]. This opens up exciting opportunities for the study of the anisotropy of the Dirac cone. Up to now, to the best of our knowledge, no rectangular material except for 6,6,12-graphyne has been explored in 2D carbon allotropes. Therefore, to study the anisotropy of Dirac cones, particularly in rectangular lattices, is timely.

In this letter, we focus the attention on the anisotropy of the Dirac cone in rectangular 2D carbon allotropes. In addition, the anisotropy is demonstrated to be tunable through changing the lattice parameters or the lattice ratios. The changing of lattice parameters and lattice ratios is achieved by inserting certain -C≡C- linkages into the carbon bonds in 6,6,12-graphyne. Three typical derivates are involved, which are called 6,6,18-graphdiyne, 6,6,24-graphtriyne, and hybrid(h)-12,12,20-graphdyne-grapdiyne(graphdy(i)ne), as illustrated in fig. 1. As the electron's wave function moves through momentum space, the charge carriers can be seen propagating along certain preferred crystalline directions in the vicinity of Dirac points, which obeys the anisotropy of Dirac cones. We show that, in all the cases considered, the rectangular symmetry of the carbon allotropes leads to the anisotropy of Dirac cones. Furthermore, the lattice parameters as well as the lattice ratio can be used to tune this anisotropy. When the Dirac cone is far away from the high-symmetry points, the direction-dependent Dirac cone has a threefold-like symmetry, and the anisotropy of Dirac cone is close to 70%. Our findings will provide the platform for the future exploration of the anisotropy of the Dirac cone as an information carrier [15].

Our calculations are carried out based on the density functional theory (DFT), which is implemented in the SIESTA package [31]. The generalized gradient approximation Perdew-Burke-Ernzerhof (PBE) exchange-correlation functional [32] and norm-conserving pseudopotentials [33] are selected in the calculations. In order to get energy levels degenerate at Dirac points, a large mesh cutoff of 400 Ry is required. The optimized double-ζ orbitals including polarization orbitals are employed to describe the valence electrons. $21 \times 21 \times 1$ and $31 \times 31 \times 1$ are used for the Monkhorst-Pack k-point mesh of geometry optimization and self-consistent calculation, respectively. The conjugate gradient algorithm is adopted to fully relax the geometry until the force on any individual atom is less than 0.005 eV/Å.

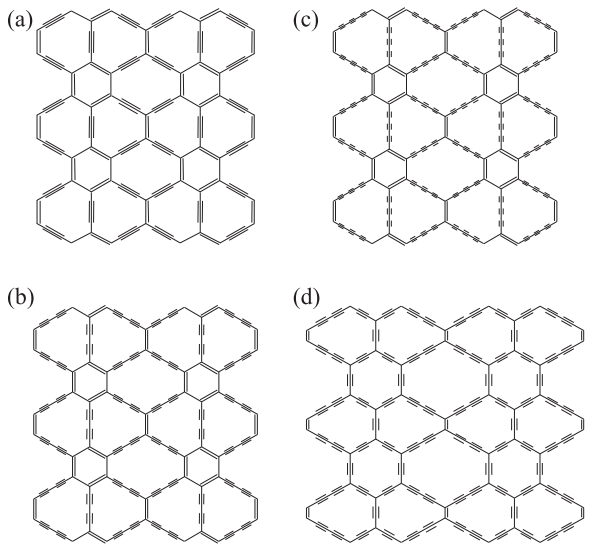

Fig. 1: Four typical 2D carbon allotropes with the rectangular lattice. (a) 6,6,12-graphyne. (b) 6,6,18-graphdiyne. (c) 6,6,24-graphtriyne. (d) h-12,12,20-graphy(i)ne.

As a solid check, we first calculate the band structure and Dirac cones of 6,6,12-graphyne. All results obtained in our simulations are in agreement with the previous work [11] (not shown for brevity). In contrast to 6,6,12-graphyne, the three carbon rings (denoted as 6, 6, and 12) are connected by -C≡C-C≡C- instead of -C≡C- linkages in 6,6,18-graphdiyne. This is the reason why we designate it 6,6,18-graphdiyne as the three carbon rings 6, 6, and 18 are connected by the diacetylenic linkages in 6,6,18-graphdiyne. The designation used in this work is the same as in the literature [34]. Although 6,6,18-graphdiyne and 6,6,12-graphyne share the same rectangular lattice, the band structures are in different manners. Two Dirac points are detectable in 6,6,12-graphyne: one (Dirac point I) is along the Γ-X' line and close to the X' point, and the other (Dirac point II) appears along the M-X line and is very near the X-point [11]. However, in the case of 6,6,18-graphdiyne, Dirac points degenerate into one, as indicated from the band structure in fig. 2(a). The Dirac point along the line from Γ to X' points remains intact, but the one located on the line from M to X disappears. Unlike the four Dirac cones of 6,6,12-graphyne in the Brillouin zone, 6,6,18-graphdiyne only has two Dirac points which are related by symmetry. The Dirac point of 6,6,18-graphdiyne is closer to the X'-point compared to the Dirac point I of 6,6,12-graphyne. This stems from the larger lattice parameters and the lattice ratio $a/b = 1.47$ (see table 1 for more details). On the other hand, the Dirac point along the M-X line is delocalized

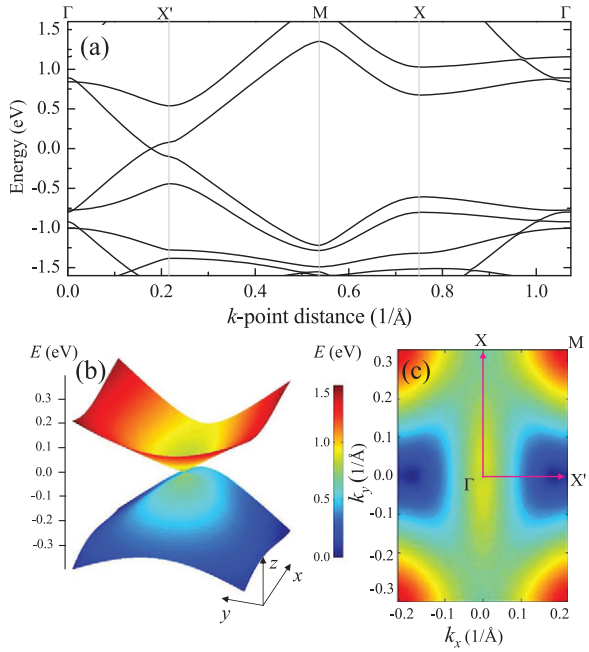

Fig. 2: (Color online) Electronic structure of 6,6,18-graphdiyne. (a) Band structure. The Fermi level is set at 0 eV. (b) 3D Dirac cone. (c) The lowest unoccupied band projected onto the first Brillouin zone in terms of contour plots.

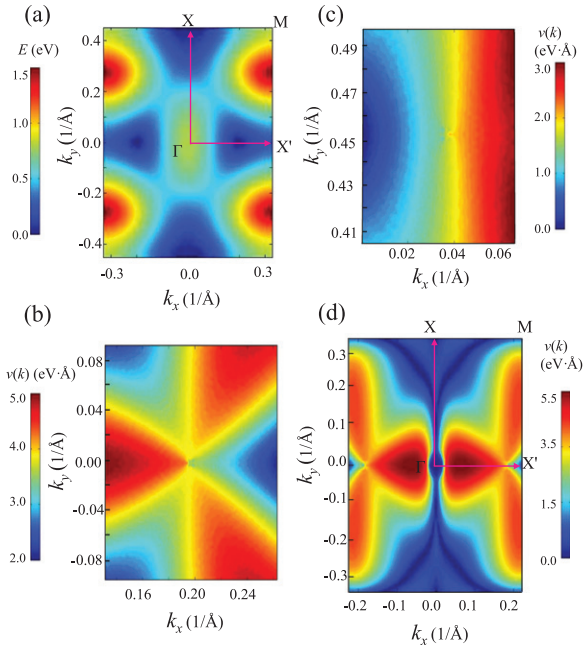

Fig. 3: (Color online) (a) The lowest unoccupied band projected onto the first Brillouin zone for 6,6,12-graphyne. The corresponding group velocities with respect to Dirac points in the vicinity of Dirac points I (b) and II (c). (d) The group velocities with respect to the Dirac points for 6,6,18-graphdiyne in the entire first Brillouin zone.

Table 1: The optimized lattice parameters (in units of Å) of four rectangular lattices. The lattice ratios and the anisotropies are given as well.

Name	a	b	a/b	$\mathcal{A}$
6,6,12-graphyne	9.54	6.96	1.37	33%*
6,6,12-graphyne	9.54	6.96	1.37	39%†
6,6,18-graphdiyne	14.07	9.57	1.47	70%
6,6,24-graphtriyne	18.60	12.19	1.52	56%
h-12,12,20-graphy(i)ne	18.61	12.23	1.52	40%

* Dirac cone I.

† Dirac cone II.

and thus is more easily affected by the changes going from 6,6,12-graphyne to 6,6,18-graphdiyne [12]. As an additional -C≡C- linkage is inserted, the hopping parameters are changed accordingly and the corresponding balance between these hopping energies is also broken. Such a mutual competition between the effective parameters results in the absence of the Dirac point along the M-X line in 6,6,18-graphdiyne [29].

In fig. 2(b), we plot a 3D representation of the Dirac cone in the vicinity of the Fermi level for 6,6,18-graphdiyne. Our finding is very insightful. The anisotropic Dirac cone is obvious and looks like an egg near the Fermi energy level. This is a striking difference from the graphene-like materials with the triangular lattice [2,11,35], where the projections of the Dirac cone on the Brillouin zone are circles in the vicinity of Dirac points.

To further understand the momentum-dependent nature of the Dirac cone in 6,6,18-graphdiyne, we project the lowest unoccupied band onto the first Brillouin zone, as displayed in fig. 2(c). We note in passing that the projected highest occupied band has a similar fashion. It explicitly demonstrates that the anisotropy of the Dirac cone in 6,6,18-graphdiyne is generic. Roughly speaking, the energy-momentum change along the k_x-direction is lower than that along the k_y-direction, indicating that the charge carriers prefer to propagate along the k_x-direction with a lower energy barrier. This is the direct manifestation of the crystal momentum-dependent anisotropy of the Dirac cone.

We should point out that the charge carriers move through momentum space, which can be well described by the group velocities of charge carrier. As Dirac cones are anisotropic in the rectangular lattices, the motion of charge carriers largely depends on the crystalline direction. Therefore, we define the anisotropy of Dirac cones as

$$\mathcal{A}[v(\mathbf{k})] = \frac{\max v(\mathbf{k}) - \min v(\mathbf{k})}{\max v(\mathbf{k})} \qquad (1)$$

by considering the maximum and minimum velocities of charge carriers with respect to the Dirac point in the momentum space. As the normalized denominator is used in eq. (1), the value $\mathcal{A} = 1$ is referred to the largest anisotropy while the value $\mathcal{A} = 0$ gives no anisotropy.

In 6,6,12-graphyne, the anisotropy of Dirac cones I and II exists, which is presented clearly from the projected

lowest unoccupied band in the first Brillouin zone, as shown in fig. 3(a). In the case of the Dirac cone I as shown in fig. 3(b), the anisotropy behaves as a threefold-like symmetry. There are three regions which have relatively larger velocities (represented in red color). The largest velocity distributes along the $-k_x$-direction and its value is around 4.5 eVÅ. Note that the parameter 2π is used in the calculations of reciprocal lattice vectors. Thus, the obtained values can be not directly compared with that reported by Malko and coworkers [11]. The other two large velocity regions are at around $\pm 45°$ with respect to the k_x-direction. The corresponding group velocities are slightly lower than that along the $-k_x$-direction. More importantly, six constant-velocity lines are detectable (yellow color), which have a velocity of ∼3.9 eVÅ. Two of them are straight lines along the $\pm k_y$-direction, which coincides with that reported by Malko *et al.* [11]. The other four are slightly curved, which are lacking in the literature [11]. As these six lines have constant velocities, zero curvatures are a natural consequence. By contrast, three regions possess the relatively lower group velocities. The lowest one is along the k_x-direction, which has a velocity of around 3.0 eVÅ. The other two are along the $\pm 135°$ directions with respect to the k_x-direction. Based on these values, we can easily obtain the anisotropy of the Dirac cone I, $\mathcal{A} = (4.5 - 3.0)/4.5 \approx 33\%$. This value is gigantic compared to the zero anisotropy in graphene-like materials.

In contrast to the Dirac cone I, the anisotropy of the Dirac cone II for 6,6,12-graphyne has a lower symmetry. As can be seen in fig. 3(c), in the vicinity of the Dirac point the carrier velocities are separated into two regions by the constant-velocity lines along the $\pm k_y$-directions. One region with the larger velocity distributes at the k_x-direction from the Dirac point, while the other one with the lower velocity locates at the $-k_x$-direction from the Dirac point. The calculated maximum and minimum velocities are around 2.5 and 1.5 eVÅ, respectively. Therefore, the anisotropy of the Dirac cone II is $\mathcal{A} = (2.5 - 1.5)/2.5 \approx 39\%$, which is slightly larger than that of the Dirac cone I. This implies that the anisotropies of Dirac cones are different even in the same material. It should be noted that there are only two lines instead of six with constant velocities for the Dirac cone II. The constant group velocities are ∼1.8 eVÅ, which agrees with what obtained by Malko *et al.* [11].

Next, we turn to 6,6,18-graphdiyne, which has larger lattice parameters and lattice ratio compared to 6,6,12-graphyne. These changes have a big effect not only on the number of Dirac cones (as described above), but also on the anisotropy of Dirac cone. In order to understand the nature of anisotropy in 6,6,18-graphdiyne, we map the group velocities with respect to the Dirac points in the entire first Brillouin zone, as displayed in fig. 3(d). In the vicinity of Dirac points, the group velocities have a similar character to the Dirac cone II of 6,6,12-graphyne and appear as a threefold-like symmetry. The maximum velocity is along the $-k_x$-direction with a value of

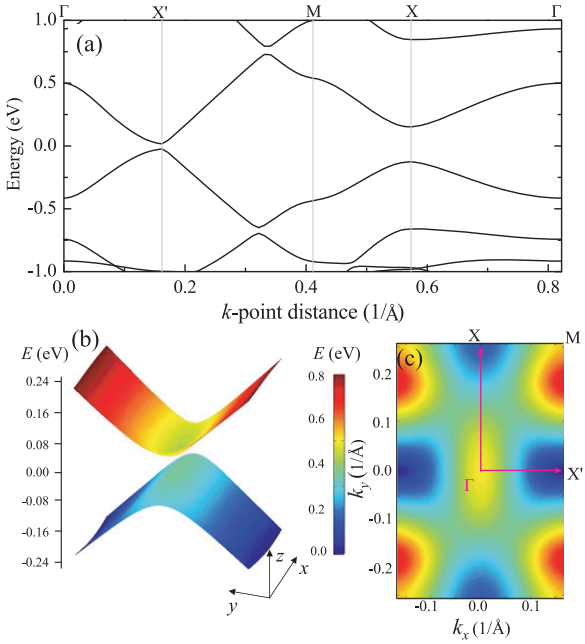

Fig. 4: (Color online) Electronic structure of 6,6,24-graphtriyne. (a) Band structure. The Fermi level is chosen to be 0 eV. (b) 3D Dirac cone. (c) The lowest unoccupied band projected onto the first Brillouin zone in terms of contour plots.

5.0 eVÅ, while the minimum velocity appears along the k_x-direction and is ∼1.5 eVÅ. As a result, the calculated anisotropy has a value $\mathcal{A} = (5.0 - 1.5)/5.0 \approx 70\%$ for 6,6,18-graphdiyne. This is about two orders of magnitude larger than the values in 6,6,12-graphyne, which arise from the larger lattice parameters, especially the larger lattice ratio. Accordingly, the anisotropy of Dirac cone is tuned through changing the lattice parameters as well as the lattice ratio. Future experiments can test this prediction directly. More intriguingly, two obvious lines with constant velocities are observed, which are at around $\pm 45°$ with respect to the k_x-direction. But they are no longer the straight lines. The corresponding group velocities are ∼3.4 eVÅ, which are slightly larger than the values for 6,6,12-graphyne.

If we use the triacetylenic (-C≡C-C≡C-C≡C-) linkages to replace the -C≡C-C≡C- linkages in the turning of 6,6,12-graphyne into 6,6,18-graphdiyne, 6,6,24-graphtriyne is derived, as shown in fig. 1(c). Due to the much larger lattices as well as the much larger lattice ratio $a/b = 1.52$, an immediate change emerges in the band structure. As can be seen in fig. 4(a), a tiny band gap of ∼0.04 eV opens at the Dirac point and locates more closely to the X' point compared to the case of 6,6,18-graphdiyne. Thus, an applied external electric field can manipulate such material-based devices efficiently as the carrier becomes massive. Although the reflection symmetry breaking is ascribed to the tiny band gap opened in 6_{BN},6,12-graphyne [12], it is not

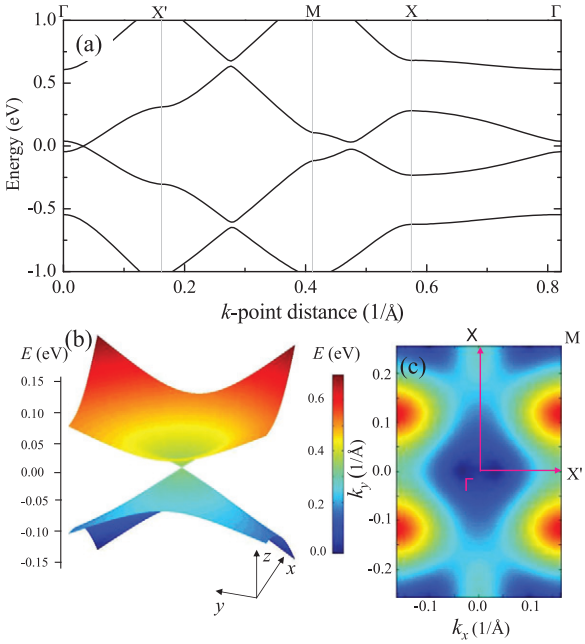

Fig. 5: (Color online) Electronic structure of h-12,12,20-graphy(i)ne. (a) Band structure. The Fermi level is chosen to be 0 eV. (b) 3D Dirac cone. (c) The lowest unoccupied band projected onto the first Brillouin zone in terms of contour plots.

the case in 6,6,24-graphtriyne. The underlying mechanism originates from the larger lattice parameters and the subsequently weakened coupling strength between lattice sites as well as the changed hopping energies [13,29]. If we take an alternative way to insert the additional -C≡C- linkage into 6,6,18-graphdiyne, another carbon allotrope called h-12,12,20-graphy(i)ne is obtained, as illustrated in fig. 1(d). Interestingly, although 6,6,24-graphtriyne and h-12,12,20-graphy(i)ne possess almost identical lattice parameters and lattice ratios, their band structures are quite different. In contrast to 6,6,24-graphtriyne, h-12,12,20-graphy(i)ne has a gapless Dirac cone, which is along the Γ-X' line close to the Γ-point, as shown in fig. 5(a).

In 6,6,24-graphtriyne, the Dirac point is very close to the X'-point. The group velocities with respect to the Dirac points are plotted in the entire first Brillouin zone, as displayed in fig. 6(a). As can be seen, the charge carriers will very soon meet a larger barrier along the k_y-direction compared to the motion along the k_x-direction. The maximum velocity reaches around 4.1 eVÅ, while the minimum is only around 1.8 eVÅ. The anisotropy of Dirac cones is estimated to be $\mathcal{A} = (4.1 - 1.8)/4.1 = 56\%$ for 6,6,24-graphtriyne. It is slightly smaller than the value in 6,6,18-graphdiyne, but still larger than that in 6,6,12-graphyne. As for h-12,12,20-graphy(i)ne, in the vicinity of the Dirac point the group velocities behave as a twofold-like symmetry. Figure 6(b) clearly shows that the charge carrier has a maximum velocity of 2.5 eVÅ, which is at around ±45° with respect to the k_x-direction. The minimum velocity

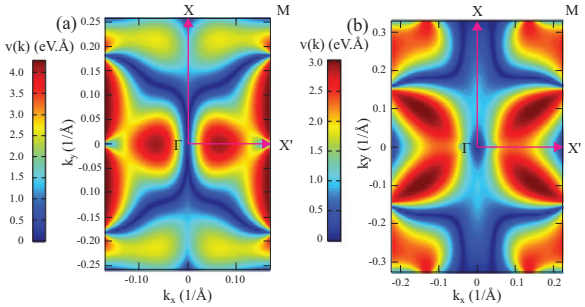

Fig. 6: (Color online) The group velocities with respect to the Dirac points for (a) 6,6,24-graphtriyne and (b) h-12,12,20-graphy(i)ne in the entire first Brillouin zone.

has a value of 1.5 eVÅ and is along the $-k_x$-direction. The corresponding anisotropy is $\mathcal{A} = (2.5 - 1.5)/2.5 = 40\%$. This value is nearly equal to that in 6,6,12-graphyne even if they have different lattice parameters. However, it is still smaller than that of 6,6,24-graphtriyne although they possess the same lattice parameters and lattice ratio. The detailed values of anisotropy in these four carbon allotropes are summarized in table 1. In addition, we note that the Dirac anisotropy may lead to an anisotropy of resistance in experiment [36], which will broaden its potential uses in information applications.

In conclusion, the anisotropy of Dirac cones are studied in the rectangular carbon allotropes using an *ab initio* method. The results suggest the possibility to manipulate the anisotropy of Dirac cones by varying the lattice parameters as well as the lattice ratio. Among these four carbon allotropes studied, 6,6,18-graphdiyne yields the largest anisotropy of 70%. Once these materials are successfully synthesized in experiments, they absolutely will play a role in information applications. This is because the anisotropy of Dirac cones can be regarded as an information carrier in the momentum space.

* * *

This work was supported by the National Basic Research Program of China under Grant No. 2012CB933101 and the National Science Foundation under Grant Nos. 11104122, 51372107. MSS thanks the State Scholarship Fund by the China Scholarship Council for financially supporting his visit to Indiana State University. We would like to thank Zhiya Zhang (LZU) for valuable discussions.

REFERENCES

[1] Castro Neto A. H., Guinea F., Peres N. M. R., Novoselov K. S. and Geim A. K., *Rev. Mod. Phys.*, **81** (2009) 109.
[2] Niu X., Mao X., Yang D., Zhang Z., Si M. and Xue D., *Nanoscale Res. Lett.*, **8** (2013) 469.
[3] Geim A. K. and Novoselov K. S., *Nat. Mater.*, **6** (2007) 183.

[4] Katsnelson M. I., Novoselov K. S. and Geim A. K., *Nat. Phys.*, **2** (2006) 620.
[5] Pathak S., Shenoy V. B. and Baskaran G., *Phys. Rev. B*, **81** (2010) 085431.
[6] Gusynin V., Sharapov S. and Carbotte J., *Phys. Rev. Lett.*, **96** (2006) 256802.
[7] Bolotin K. I., Sikes K. J., Hone J., Stormer H. L. and Kim P., *Phys. Rev. Lett.*, **101** (2008) 096802.
[8] Novoselov K. S., Geim A. K., Morozov S. V., Jiang D., Zhang Y., Dubonos S. V., Grigorieva I. V. and Firsov A. A., *Science*, **306** (2004) 666.
[9] Bostwick A., Ohta T., Seyller T., Horn K. and Rotenberg E., *Nat. Phys.*, **3** (2007) 36.
[10] Wang J.-R. and Liu G.-Z., *Phys. Rev. B*, **89** (2014) 195404.
[11] Malko D., Neiss C., Viñes F. and Görling A., *Phys. Rev. Lett.*, **108** (2012) 086804.
[12] Malko D., Neiss C. and Görling A., *Phys. Rev. B*, **86** (2012) 045443.
[13] Peng J., Fu Z.-G. and Li S.-S., *Appl. Phys. Lett.*, **101** (2012) 222108.
[14] Chong Y., *Nature*, **496** (2013) 173.
[15] Moore J. E., *Nature*, **464** (2010) 194.
[16] Tang S. and Dresselhaus M. S., *Nano Lett.*, **12** (2012) 2021.
[17] Richard P., Nakayama K., Sato T., Neupane M., Xu Y.-M., Bowen J. H., Chen G. F., Luo J. L., Wang N. L., Dai X., Fang Z., Ding H. and Takahashi T., *Phys. Rev. Lett.*, **104** (2010) 137001.
[18] Huang X., Lai Y., Hang Z. H., Zheng H. and Chen C. T., *Nat. Mater.*, **10** (2011) 582.
[19] Bravo-Abad J., Joannopoulos J. D. and Soljacic M., *Proc. Natl. Acad. Sci. U.S.A.*, **109** (2012) 9761.
[20] Rechtsman M. C., Zeuner J. M., Plotnik Y., Lumer Y., Podolsky D., Dreisow F., Nolte S., Segev M. and Szameit A., *Nature*, **464** (2013) 196.
[21] Feng Y., Wang Z., Chen C., Shi Y., Xie Z., Yi H., Liang A., He S., He J., Peng Y., Liu X., Liu Y., Zhao L., Liu G., Dong X., Zhang J., Chen C., Xu Z., Dai X., Fang Z. and Zhou X. J., *Sci. Rep.*, **4** (2014) 5385.
[22] Choi S.-M., Jhi S.-H. and Son Y.-W., *Phys. Rev. B*, **81** (2010) 081407(R).
[23] Wang G., Si M., Kumar A. and Pandey R., *Appl. Phys. Lett.*, **104** (2014) 213107.
[24] Park C.-H., Yang L., Son Y.-W., Cohen M. L. and Louie S. G., *Nat. Phys.*, **4** (2008) 213.
[25] Dietl P., Piéchon F. and Montambaux G., *Phys. Rev. Lett.*, **100** (2008) 236405.
[26] Pardo V. and Pickett W. E., *Phys. Rev. Lett.*, **102** (2009) 166803.
[27] Banerjee S., Singh R. R. P., Pardo V. and Pickett W. E., *Phys. Rev. Lett.*, **103** (2009) 016402.
[28] Volovik G. E., *JETP Lett.*, **73** (2001) 162.
[29] Huang H., Duan W. and Liu Z., *New J. Phys.*, **15** (2013) 023004.
[30] Li G., Li Y., Liu H., Guo Y., Li Y. and Zhu D, *Chem. Commun.*, **46** (2010) 3256.
[31] Artacho E., Anglada E., Diéguez O., Gale J. D., García A., Junquera J., Martin R. M., Ordejón P., Pruneda J. M., Sánchez-Portal D. and Soler J. M., *J. Phys.: Condens. Matter*, **20** (2008) 064208.
[32] Perdew J. P., Burke K. and Ernzerhof M., *Phys. Rev. Lett.*, **77** (1996) 3865.
[33] Troullier N. and Martins J. L., *Phys. Rev. B*, **43** (1991) 1993.
[34] Baughman R. H., Eckhardt H. and Kertesz M., *J. Chem. Phys.*, **87** (1987) 6687.
[35] Deng X., Si M. and Dai J., *J. Chem. Phys.*, **137** (2012) 201101.
[36] Kim K. S., Zhao Y., Jang H., Lee S. Y., Kim J. M., Kim K. S., Ahn J.-H., Kim P., Choi J.-Y. and Hong B. H., *Nature*, **457** (2009) 706.